Joint Optimization of Beam-Hopping Design and NOMA-Assisted Transmission for Flexible Satellite Systems

Anyue Wang, *Graduate Student Member, IEEE*, Lei Lei, *Member, IEEE*, Eva Lagunas, *Senior Member, IEEE*, Ana I. Pérez-Neira, *Fellow, IEEE*, Symeon Chatzinotas, *Senior Member, IEEE*, and Björn Ottersten, *Fellow, IEEE*

***Abstract*— Next-generation satellite systems require more flexibility in resource management such that available radio resources can be dynamically allocated to meet time-varying and non-uniform traffic demands. Considering potential benefits of beam hopping (BH) and non-orthogonal multiple access (NOMA), we exploit the time-domain flexibility in multi-beam satellite systems by optimizing BH design, and enhance the power-domain flexibility via NOMA. In this paper, we investigate the synergy and mutual influence of beam hopping and NOMA. We jointly optimize power allocation, beam scheduling, and terminal-timeslot assignment to minimize the gap between requested traffic demand and offered capacity. In the solution development, we formally prove the NP-hardness of the optimization problem. Next, we develop a bounding scheme to tightly gauge the global optimum and propose a suboptimal algorithm to enable efficient resource assignment. Numerical results demonstrate the benefits of combining NOMA and BH, and validate the superiority of the proposed BH-NOMA schemes over benchmarks.**

***Index Terms*— Multi-beam satellite systems, beam hopping, non-orthogonal multiple access, resource optimization.**

I. Introduction

IN CONVENTIONAL multi-beam satellite systems, all beams are simultaneously illuminated and on-board resources are pre-assigned before launch due to limited flexibility and capability in satellite payloads [1]. While this design is efficient for static and uniform traffic patterns, the evolution of data services leads to highly dynamic and spatially non-uniform traffic. In this case, the efficiency of resource utilization is low and the system fails to adapt to heterogeneous traffic distribution over the coverage area [2]. With the development of advanced satellite payloads, more attention has been drawn to flexible on-board resource allocation (e.g., power, bandwidth) to embrace the dramatic growth of data traffic and the uneven traffic distribution [2], [3].

Beam hopping (BH) is a promising technique to enhance the flexibility of resource management by selectively and sequentially activating or deactivating beams [2], [4], [5]. The benefits of BH are from the following aspects. First, in a BH system, beam scheduling (or beam illumination pattern design) is optimized based on the requested traffic such that unmet and unused capacity can be reduced [4], [5]. Second, without illuminating all the beams together, the required number of radio-frequency chains is smaller, thus power consumption and payload mass are reduced [5]. Third, spatially induced co-channel interference can be alleviated by illuminating the beams that are distant from each other [6], [7]. In the DVB-S2X standard [8], a super-frame format to facilitate BH implementation and performance enhancement has been specified. In the literature, BH has been applied in different scenarios, e.g., load balancing networks [9], cognitive satellite networks [10], and ultra-dense LEO systems [11].

A. Related Works

To improve the performance of BH, a majority of works focus on how to design efficient approaches to decide beam-timeslot scheduling. In [4], a genetic algorithm was adopted to determine beam illumination patterns. In [10], a resource allocation problem for cognitive BH systems was studied. The authors decomposed the problem and proposed low-complexity approaches. In [12], the authors designed two iterative BH approaches based on minimum co-channel interference and maximum signal-to-interference-plus-noise ratio (SINR). The authors in [13] studied resource allocation for a novel satellite system where conventional BH is combined

Manuscript received 13 October 2021; revised 28 February 2022; accepted 14 April 2022. Date of publication 5 May 2022; date of current version 11 October 2022. This work was supported in part by the Luxembourg National Research Fund (FNR) CORE Project Resource Optimization for integrated Satellite-5G nETworks with non-orThogonal multiple Access (ROSETTA) under Grant C17/IS/11632107 and in part by Resource Optimization for Next Generation of Flexible SATellite Payloads (FlexSAT) under Grant C19/IS/13696663. An earlier version of this work was presented at the 2021 IEEE Wireless Communications and Networking Conference (WCNC) [21] [DOI: 10.1109/WCNC49053.2021.9417306]. The associate editor coordinating the review of this article and approving it for publication was Y.-F. Liu. *(Corresponding author: Lei Lei.)*

Anyue Wang, Eva Lagunas, Symeon Chatzinotas, and Björn Ottersten are with the Interdisciplinary Center for Security, Reliability and Trust, University of Luxembourg, 4365 Esch-sur-Alzette, Luxembourg (e-mail: anyue.wang@uni.lu; eva.lagunas@uni.lu; symeon.chatzinotas@uni.lu; bjorn.ottersten@uni.lu).

Lei Lei is with the School of Information and Communications Engineering, Xi'an Jiaotong University, Xi'an 710049, China (e-mail: lei.lei@xjtu.edu.cn).

Ana I. Pérez-Neira is with the Centre Tecnològic de Telecomunicacions de Catalunya (CTTC/CERCA), 08860 Castelldefels, Spain, and also with the Department of Signal Theory and Communications, Universitat Politècnica de Catalunya (UPC), 08034 Barcelona, Spain (e-mail: ana.perez@cttc.es).

Color versions of one or more figures in this article are available at https://doi.org/10.1109/TWC.2022.3170435.

Digital Object Identifier 10.1109/TWC.2022.3170435

This work is licensed under a Creative Commons Attribution 4.0 License. For more information, see https://creativecommons.org/licenses/by/4.0/

with cluster hopping. Considering the benefits of machine learning techniques, the authors in [14] and [15] proposed resource allocation schemes assisted by deep reinforcement learning and deep learning, respectively.

Compared to conventional orthogonal multiple access (OMA), non-orthogonal multiple access (NOMA) can achieve higher spectral efficiency and serve more terminals [16]. Beyond terrestrial systems, it is natural to investigate how NOMA can help to improve the performance for multi-beam satellite systems, e.g., [17]–[20]. The authors in [17] studied the cooperation between NOMA and precoding in a multi-beam satellite system. In [18], joint optimization of power allocation, decoding orders, and terminal-timeslot assignment in NOMA-enabled multi-beam satellite systems was studied. To mitigate channel-phase uncertainty effects, two robust beamforming schemes were provided in [19] to minimize power consumption for delivering satellite internet-of-things services. In [20], the authors jointly optimized power allocation and network stability to maximize long-term average capacity for NOMA-based satellite internet-of-things systems. NOMA has shown superiorities in enhancing spectral efficiency and improving the performance of practical metrics for multi-beam satellite systems in the literature.

Considering the individual benefits from BH and NOMA, we are motivated to investigate how to exploit the joint advantages of these two techniques and optimize resource allocation for BH-NOMA systems. In the literature, the joint scheme of BH and NOMA is studied to a limited extent. The potential synergies of NOMA and BH were firstly studied in our previous work [21], where we considered a simplified problem and focused on performance evaluation in order to verify the initial synergy between BH and NOMA.

B. Motivations and Contributions

In general, joint resource optimization for BH-NOMA systems typically leads to a combinatorial optimization problem. In some cases, the optimum might not be achievable for large-scale instances due to unaffordable complexity and time, e.g., branch-and-bound approach in solving large-scale integer linear programming problems [15], [22]. For some difficult problems, the optimum might even be unknown for small or medium cases, e.g., unknown optimum in solving mixed-integer non-convex programming (MINCP) problems [21]. It is therefore of importance to: 1) Identify how difficult the resource optimization problem is; 2) Provide a tight bound for the optimum; 3) Properly benchmark the developed suboptimal solutions.

In this paper, we investigate joint optimization for the considered BH-NOMA scheme to enhance the performance gain by optimizing power allocation, beam scheduling, and terminal-timeslot assignment. We apply BH to selectively and sequentially activate beams over timeslots. NOMA is then implemented within each active beam to further improve the spectral efficiency. We aim at minimizing the gap between offered capacity and requested traffic, which is a practical and widely-adopted metric to capture capacity-demand mismatches for satellite systems [3], [7]. Considering the benefits of higher spectral efficiency and more flexibilities in resource allocation than OMA, NOMA can improve the capacity for terminals with unmet capacity such that the capacity-demand gap can be further reduced. Beyond state-of-the-art and compared to [21], the main contributions are summarized as follows:

- We formulate a resource allocation problem to minimize the gap between offered capacity and requested traffic, leveraging by BH and NOMA. The work, together with [21], provides an early-attempt investigation for BH-NOMA systems.
- We formally prove the NP-hardness of the joint BH-NOMA optimization problem and outline the mutual influence between BH and NOMA. We investigate the problem's insights by developing theoretical analysis.
- To gauge the unknown global optimum, we design an effective bounding scheme. In the upper-bound approach (UBA), we develop an iterative near-optimal algorithm. In the lower-bound approach (LBA), we first resolve the problem's non-convexity by simplifying the estimation of inter-beam interference. Then we construct a mixed-integer conic programming (MICP) problem to approximate the original problem.
- We design an efficient suboptimal algorithm for joint power allocation, beam scheduling, and terminal-timeslot assignment (E-JPBT) to overcome the high complexity in UBA and provide feasible solutions for large-scale instances.
- The numerical results validate the benefits of jointly considering BH and NOMA, and the tightness of the bounds in gauging optimality. We demonstrate the superiority of the proposed BH-NOMA schemes in matching offered capacity to requested traffic compared to benchmarks.

The remainders of the paper are organized as follows: A multi-beam system model with the coexistence of BH and NOMA is illustrated in Section II. In Section III, we formulate a joint resource optimization problem and provide theoretical analysis of the problem. The procedures of UBA and LBA are elaborated in Section IV and Section V, respectively. In Section VI, we present the details of designing E-JPBT. The performance of the proposed algorithms is evaluated and discussed in Section VII. Section VIII concludes the paper.

Some notations are defined as follows: The operator $|\cdot|$ denotes the absolute value of a complex number or the cardinality of a set. $f(x;y)$ represents the function $f(x,y)$ with given y. $[x]^+$ is equivalent to the calculation of $\max\{x,0\}$. The operation of $\mathcal{X}\times\mathcal{Y}=\{(x,y)|x\in\mathcal{X},y\in\mathcal{Y}\}$ denotes the Cartesian product of two sets.

II. System Model

We consider a geostationary earth orbit (GEO) satellite system which provides services to fixed ground terminals via forward links. The satellite generates B spot beams to cover the targeted area. We denote $\mathcal{B}$ as the set of the beams. Let $\mathcal{K}$ and $\mathcal{K}_b$ represent the set of terminals in the system and in the b-th beam, respectively. Note that terminals are assigned to

beams implicitly based on their geographical coordinates [23], e.g., terminal k located within the 4.3 dB contour of the b-th beam's coverage area belonging to $\mathcal{K}_b$. Denote K' as the number of terminals per beam. Each terminal is equipped with a single directional antenna. All the beams share the same frequency band, i.e., 1-color frequency-reuse pattern.

The architecture of the considered multi-beam satellite system is depicted in Fig. 1, where the telemetry, tracking, and command (TT&C) station is part of the satellite operation center whereas the gateway and the resource manager are part of the network operation center [2]. The TT&C station is responsible for the synchronization among beams during the BH process [24]. The bent-pipe transparent satellite payload is assumed to be equipped with switching matrix and digital transparent processors to enable beam activation/deactivation and power distribution among different active beams, respectively [1], [2]. The procedure in Fig. 1 is described as the following: Step 1: The gateway collects information from ground terminals, e.g., traffic demand and channel status, via return links. Step 2: Based on the feedbacks, the resource manager (co-located with the gateway) executes the algorithm to optimize the beam illumination pattern and power-terminal-timeslot scheduling. The optimization outcomes are communicated to the satellite payload via the TT&C station and to the gateway [2], [15]. Step 3: Following the planned scheduling decisions, the gateway requests data from the core networks to the satellite payload. Step 4: According to the optimized beam illumination pattern, the satellite payload relies on a switching matrix to activate the selected beams. The satellite payload delivers data to the ground terminals in active beams.

In the system, BH illuminates no more than B_0 ($B_0 < B$) beams at each timeslot due to payload architecture limitations. A scheduling period consists of T timeslots, defined as a BH window. Denote $\mathcal{T}$ as the set of the timeslots. For each beam, $\left\lceil \frac{K'}{K_0} \right\rceil$ timeslots are required such that all the terminals can be scheduled to at least one timeslot. The minimum number of timeslots to illuminate all the beams at least once is $\left\lceil \frac{B}{B_0} \right\rceil$. Thus the value of T should meet $T \geq \left\lceil \frac{K'}{K_0} \right\rceil \left\lceil \frac{B}{B_0} \right\rceil$. In an active beam, NOMA is adopted to multiplex one or more terminals in a timeslot. The signals intended for the scheduled terminals in one beam are superimposed with different power per targeted terminal. We denote p_{kt} as the transmit power for terminal k at timeslot t. The SINR of terminal k in beam b at timeslot t is derived as,

$$\gamma_{kt} = \frac{|h_{bk}|^2 p_{kt}}{\underbrace{\sum_{\substack{k' \in \mathcal{K}_b \setminus \{k\} \\ k' < k}} |h_{bk}|^2 p_{k't}}_{\text{intra-beam interference}} + \underbrace{\sum_{b' \in \mathcal{B} \setminus \{b\}} \sum_{k' \in \mathcal{K}_{b'}} |h_{b'k}|^2 p_{k't}}_{\text{inter-beam interference}} + \sigma^2}, \tag{1}$$

where σ^2 represents the noise power. We denote $|h_{bk}|^2$ as the channel gain from the b-th satellite antenna to the k-th terminal (assuming consistent indexes between antennas and beams). We use a widely-adopted channel model in multi-beam satellite systems [6], [10], [15], [18], which is derived as,

$$|h_{bk}|^2 = \frac{G_{bk}^{\text{tx}} G_k^{\text{rx}}}{\kappa T^{\text{noise}} W} \left(\frac{c}{4\pi d_k f^{\text{fr}}} \right)^2, \tag{2}$$

where G_{bk}^{tx} is the transmit antenna gain from the b-th antenna to terminal k. G_k^{rx} denotes the receive antenna gain of terminal k. The term $\kappa T^{\text{noise}} W$ represents the distribution of noise, where κ, T^{noise}, and W denote the Boltzmann constant, the noise temperature of the receiver, and the carrier bandwidth, respectively. The term $\left(\frac{c}{4\pi d_k f^{\text{fr}}} \right)^2$ is the free-space propagation loss, where d_k, f^{fr}, and c denote the distance between the satellite and terminal k, the frequency, and the light speed, respectively. We consider that the channel gains are static within T timeslots and updated every T timeslots.

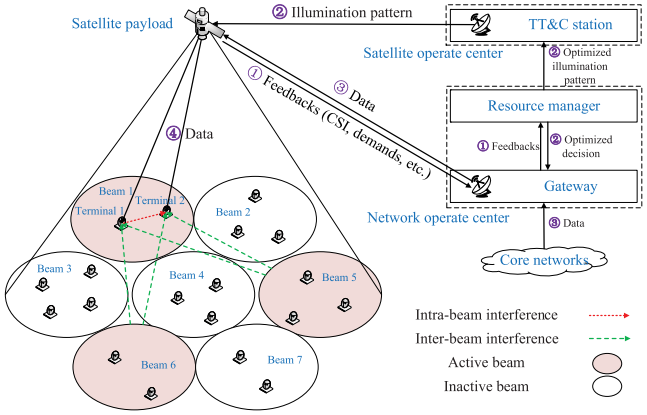


Fig. 1. An illustrative scenario of the considered BH-NOMA system. Three beams are activated simultaneously according to the BH design. By applying NOMA in beam 1, terminal 1 at the beam center with better channel gain only receives inter-beam interference from the other two active beams, while terminal 2 at the beam edge with worse channel gain receives both intra-beam and inter-beam interference. (The numbers in the circle denote the steps of the communication procedure).

The intra-beam interference and inter-beam interference are denoted as the first term and the second term of the denominator in (1), respectively. We assume consistent indexes between terminals and the descending order of channel gains, e.g., two terminals k and k' in $\mathcal{K}_b$, where $k' < k$ and $|h_{bk'}|^2 > |h_{bk}|^2$. In this case, k' performs successive interference cancellation (SIC) to decode and remove k's signals whereas k treats k''s signals as noise. We remark that, to facilitate the analysis, we assume that the channel coefficients satisfy the conditions derived in [25] (Lemma 1), such that determining the decoding order in each beam is independent of the beams' transmit power and inter-beam interference. The available rate of terminal k at timeslot t is,

$$R_{kt} = W \log_2(1 + \gamma_{kt}), \tag{3}$$

where W is the bandwidth for the carrier (single carrier per beam). The total offered capacity of terminal k is,

$$R_k = \sum_{t \in \mathcal{T}} R_{kt}. \tag{4}$$

III. Problem Formulation and Analysis

A. Problem Formulation

We formulate an optimization problem to minimize the gap between offered capacity and requested traffic by jointly optimizing power allocation, beam scheduling, and terminal-timeslot assignment. The variables are defined as:

$$p_{kt} \geq 0, \quad \text{transmit power for terminal } k \text{ at timeslot } t;$$

$$\alpha_{bt} = \begin{cases} 1, & \text{beam } b \text{ is illuminated at timeslot } t, \\ 0, & \text{otherwise;} \end{cases}$$

$$\beta_{kt} = \begin{cases} 1, & \text{terminal } k \text{ is assigned to timeslot } t, \\ 0, & \text{otherwise.} \end{cases}$$

Denote D_k as the requested traffic demand (in bps) of terminal k over a scheduling period. We apply $(R_k - D_k)^2$ to measure the capacity-demand mismatch of terminal k [3], [7]. The objective function captures the average mismatch level among K terminals. The problem is formulated as:

$$\mathcal{P}_0: \quad \min_{\alpha_{bt},\beta_{kt},p_{kt}} \sum_{k\in\mathcal{K}} (R_k - D_k)^2 \tag{5a}$$

$$\text{s.t.} \sum_{k\in\mathcal{K}_b} p_{kt} \leq P, \quad \forall b \in \mathcal{B},\ \forall t \in \mathcal{T}, \tag{5b}$$

$$\sum_{b\in\mathcal{B}} \alpha_{bt} \leq B_0, \quad \forall t \in \mathcal{T}, \tag{5c}$$

$$\sum_{k\in\mathcal{K}_b} \beta_{kt} \leq K_0 \alpha_{bt}, \quad \forall b \in \mathcal{B},\ \forall t \in \mathcal{T}, \tag{5d}$$

$$p_{kt} \leq P\beta_{kt}, \quad \forall k \in \mathcal{K},\ \forall t \in \mathcal{T}, \tag{5e}$$

$$R_k \geq R_k^{\min}, \quad \forall k \in \mathcal{K}, \tag{5f}$$

$$\alpha_{bt} + \alpha_{b't} \leq 1, b \neq b', \quad \forall (b,b') \in \Omega,\ \forall t \in \mathcal{T}. \tag{5g}$$

In (5b), the total transmit power of terminals in each beam at each timeslot is no larger than the beam power budget P. In (5c), no more than B_0 beams can be illuminated at each timeslot. Constraints (5d) confine that no more than K_0 terminals in each beam can be allocated to a timeslot. No terminal will be scheduled in an inactive beam. Constraints (5e) connect p_{kt} and β_{kt}, where p_{kt} is confined to zero if $\beta_{kt} = 0$, otherwise, $p_{kt} \leq P$. In (5f), the rate of each terminal should meet the minimum-rate requirement to maintain a certain level of fairness among terminals. Usually, the minimum rate is smaller than the requested traffic demand, i.e., $R_k^{\min} < D_k$. In (5g), we introduce $\Omega \subset \mathcal{B} \times \mathcal{B}$ as a set to include all the undesired beam pairs, e.g., adjacent beams with strong interference. If a beam pair $\{b, b'\} \in \Omega$, beam b or b' can be illuminated alone or grouped with other beams, e.g., illuminating beam b and b'' in timeslot t, but beam b and b' cannot be activated together in the same timeslot because $\alpha_{bt} + \alpha_{b't} = 2$ violates (5g).

In $\mathcal{P}_0$, the performance and optimization decisions in BH and NOMA are coupled with each other. In general, jointly optimizing the two components is challenging. Determining NOMA resource allocation in each beam depends on the outcome of BH design, whereas achieving a high-quality BH scheme requires appropriate decisions from NOMA resource allocation. On the one hand, BH design is of importance to resource allocation in NOMA. When a set of inappropriate beams with strong interference are activated, this can possibly result in degraded performance, e.g., low data rates per timeslot. As a consequence, each terminal might need to be assigned with more power to satisfy its demand or scheduled to more timeslots (thus suggests more timeslots consumed in total for all the terminals), which typically leads to a more complicated problem with a larger dimension and more sensitive to the feasibility issue in NOMA.

On the other hand, the decisions made in NOMA can in its turn influence the BH design. When an optimal power and terminal-timeslot allocation can be obtained in NOMA, as a result, each active beam radiates less inter-beam interference to each other compared to a suboptimal NOMA solution, and some beams can be activated with fewer timeslots due to the higher rate achieved per timeslot, which can greatly ease the BH design. Towards an overall high-quality solution for BH-NOMA systems, it is necessary to capture this mutual dependence and iteratively improve the overall performance in algorithmic design.

B. Complexity Analysis in Solving $\mathcal{P}_0$

$\mathcal{P}_0$ is an MINCP problem [26] due to the nonlinear and nonconvex functions in (5a) and (5f), and the presence of binary variables α_{bt} and β_{kt}. Solving an MINCP can be challenging in general. We further identify the intractability of $\mathcal{P}_0$ by proving the NP-completeness for its decision-version problem (or feasibility-check problem) and the NP-hardness for the optimization problem in Lemma 1 and Theorem 1, respectively. The decision-version problem of $\mathcal{P}_0$ is defined as a true-or-false problem to check if there exists a feasible solution [27]. If the decision version of $\mathcal{P}_0$ is NP-complete, then the optimization problem $\mathcal{P}_0$ is NP-hard [28], because solving $\mathcal{P}_0$ is no easier than solving its decision version. The former needs to obtain optimal solutions, whereas the latter only needs to offer a yes-or-no answer for feasibility check.

Lemma 1: The decision-version (feasibility-check) problem of $\mathcal{P}_0$ is NP-complete.

Proof: Please refer to Appendix A. □

Based on Lemma 1, the NP-hardness of $\mathcal{P}_0$ can be therefore concluded.

Theorem 1: $\mathcal{P}_0$ is NP-hard.

Being aware of the NP-hardness of $\mathcal{P}_0$ and the coupling effects between BH and NOMA, it is challenging to solve the original problem directly. Instead, we fix the binary variables and provide theoretical analysis of how to deal with the remaining problem.

It is worth noting that, even with the fixed binary variables α_{bt} and β_{kt}, the remaining power allocation problem, shown as in $\mathcal{P}_1$, is still non-convex [26].

$$\mathcal{P}_1: \quad \min_{p_{kt}} \sum_{k\in\mathcal{K}} (R_k - D_k)^2 \tag{6a}$$

$$\text{s.t. (5b), (5f),} \tag{6b}$$

where $p_{kt} \geq 0$ for $\beta_{kt} = 1$ and $p_{kt} = 0$ for $\beta_{kt} = 0$. We introduce auxiliary variables δ_k and equivalently

convert $\mathcal{P}_1$ as,

$$\mathcal{P}_1': \quad \min_{p_{kt},\delta_k} \sum_{k\in\mathcal{K}} \delta_k^2 \tag{7a}$$

$$\text{s.t. (5b), (5f)}, \tag{7b}$$

$$-\delta_k \le R_k - D_k \le \delta_k, \quad \forall k \in \mathcal{K}. \tag{7c}$$

At the optimum, $R_k - D_k$ is equal to either $-\delta_k$ or δ_k, $\forall k \in \mathcal{K}$, where $\delta_k \ge 0$. In the following proposition, we prove that $R_k \le D_k$ at the optimum, which can simplify $\mathcal{P}_1'$.

Proposition 1: At the optimum of $\mathcal{P}_1$, $R_k \le D_k$, $\forall k \in \mathcal{K}$.

Proof: Please refer to Appendix B. □

With Proposition 1, constraints (7c) can be converted into,

$$-\delta_k \le R_k - D_k, \quad \forall k \in \mathcal{K}, \tag{8}$$

which indicates that $R_k - D_k = -\delta_k$ at the optimum. In spite of the problem conversion, we observe that solving $\mathcal{P}_1'$ remains challenging due to the nonconvexity of the logarithmic-fractional composite expressions in the R-functions [26]. A widely-adopted approach to address the fractional nonconvex function is to decouple the numerator and denominator, and transform it into a series of convex problems, e.g., Dinkelbach's transform [29], and quadratic transform [30]. Compared to conventional Dinkelbach's transform, quadratic transform has shown advantages in tackling multi-ratio fractional programming by building the equivalence of the objectives between the primal and the transformed problem [30]. Besides, quadratic transform has proven its competitiveness compared to conventional successive convex approximation method [31] in power control [30]. By applying quadratic transform [30], we convert R_{kt} from fractional format to the following,

$$\begin{aligned} &f_{kt}^R(\theta_{kt}, p_{kt}) \\ &= \log\left(1 + 2\theta_{kt}\sqrt{|h_{bk}|^2 p_{kt}} - \theta_{kt}^2\left(\sum_{\substack{k'\in\mathcal{K}_b\setminus\{k\}\\ k'<k}} |h_{bk}|^2 p_{k't}\right.\right. \\ &\quad \left.\left. + \sum_{b'\in\mathcal{B}\setminus\{b\}}\sum_{k'\in\mathcal{K}_{b'}} |h_{b'k}|^2 p_{k't} + \sigma^2\right)\right), \end{aligned} \tag{9}$$

where $\theta_{kt} \ge 0$ is the auxiliary variable. With fixed θ_{kt}, f_{kt}^R is a concave function according to the basis of convex preservation for composite functions [26]. Then $\mathcal{P}_1'$ is rewritten as the following,

$$\mathcal{P}_2: \quad \min_{\theta_{kt},p_{kt},\delta_k} \sum_{k\in\mathcal{K}} \delta_k^2 \tag{10a}$$

$$\text{s.t. (5b)}, \tag{10b}$$

$$\sum_{t\in\mathcal{T}} f_{kt}^R(\theta_{kt}, p_{kt}) \ge R_k^{\min}, \quad \forall k \in \mathcal{K}, \tag{10c}$$

$$\sum_{t\in\mathcal{T}} f_{kt}^R(\theta_{kt}, p_{kt}) - D_k \ge -\delta_k, \quad \forall k \in \mathcal{K}. \tag{10d}$$

$\mathcal{P}_2$ is nonconvex in general, but can become convex when θ_{kt} is fixed, which enables an iterative approach to optimize p_{kt} with fixed θ_{kt} by solving the convex problem and updating θ_{kt} under fixed p_{kt}.

Algorithm 1 Iterative Approach for Power Allocation

Input: feasible p_{kt} and δ_k.
1: **repeat**
2: Update θ_{kt} by (11).
3: Optimize p_{kt} and δ_k by solving $\mathcal{P}_2$.
4: **until** convergence
5: Calculate R_k by (1), (3), (4).
6: **if** there exist terminals with $R_k > D_k$ **then**
7: Solve nonlinear equations in (12).
8: **end if**
Output: optimized p_{kt}, δ_k.

IV. An Iterative Approach for Upper Bound

In this section, we propose UBA algorithm to obtain an upper bound (a feasible suboptimal solution) for $\mathcal{P}_0$. In UBA, we optimize power allocation with fixed integer variables and iteratively update beam scheduling and terminal-timeslot assignment to progressively improve the performance.

A. Power Allocation With Fixed Integer Solution

The considered iterative algorithm for solving $\mathcal{P}_2$ is summarized in Alg. 1. In each iteration, line 2 and line 3 describe the procedures of alternatively update θ_{kt} and p_{kt}, respectively, where θ_{kt} is updated with fixed power allocation and p_{kt} is optimized given θ_{kt}. With fixed p_{kt}, the optimal θ_{kt} is derived by [30],

$$\theta_{kt} = \frac{\sqrt{|h_{bk}|^2 p_{kt}}}{\sum\limits_{\substack{k'\in\mathcal{K}_b\setminus\{k\}\\ k'<k}} |h_{bk}|^2 p_{k't} + \sum\limits_{b'\in\mathcal{B}\setminus\{b\}}\sum\limits_{k'\in\mathcal{K}_{b'}} |h_{b'k}|^2 p_{k't} + \sigma^2}. \tag{11}$$

With fixed θ_{kt}, $\mathcal{P}_2$ becomes convex. The optimum can be obtained by conventional algorithms, e.g., interior-point method [32]. Based on the theoretical results in [30], we conclude that the iterative process in lines 1-4 converges to a stationary point. At the end of convergence, there may exist terminals with $\sum_{t\in\mathcal{T}} f_{kt}^R > D_k$. According to the conclusion of Proposition 1, a post process in lines 6-8 is performed for these terminals by solving the following equations,

$$R_k = D_k, \quad \forall k \in \mathcal{K}^*, \tag{12}$$

where $\mathcal{K}^*$ includes the terminals with $R_k \ge D_k$. The nonlinear equations can be solved via the Levenberg-Marquardt method [33].

The complexity of Alg. 1 mainly falls into the optimization process in line 3 and solving nonlinear equations in line 7. For optimizing p_{kt} in line 3, we apply interior-point method to solve $\mathcal{P}_2$ with the complexity of $\mathcal{O}(\psi\log(\frac{1}{\varepsilon}))$ [32], where $\psi > 0$ is the parameter for self-concordant barrier and $\varepsilon > 0$ is the precision [32]. The complexity of solving nonlinear equations in line 7 is $\mathcal{O}(\varrho^{-2})$. Here, $\varrho > 0$ satisfies $||\mathbf{J}^T\mathbf{F}|| \le \varrho$, where $\mathbf{F} = \mathbf{0}$ is the nonlinear equations and $\mathbf{J}$ is the corresponding Jacobian matrix [33]. The complexity of Alg. 1 is therefore $\mathcal{O}(\max\{N\psi\log(\frac{1}{\varepsilon}), \varrho^{-2}\})$, where N is the maximum number of iterations.

B. Beam Scheduling and Terminal-Timeslot Assignment

Next, we jointly optimize beam scheduling and terminal-timeslot assignment to improve the performance iteratively. Some approaches, e.g., exhaustive search method, or branch and bound [34], are capable of obtaining the optimal or near-optimal integer solution but at the expense of unaffordable computational complexity. To avoid exponential-time complexity, we provide a scheme based on matching theory to decrease the capacity-demand gap iteratively.

The optimization of integer solutions can be viewed as two many-to-many matching problems [35], i.e., beam-to-timeslot matching and terminal-to-timeslot matching. Define $\mathcal{M}$ and $\mathcal{N}$ as the sets containing tuples of beam-to-timeslot and terminal-to-timeslot matching, respectively. Denote $y(\mathcal{M},\mathcal{N})$ as the objective value obtained by Alg. 1 under $\mathcal{M}$ and $\mathcal{N}$, where $\mathcal{M}$ and $\mathcal{N}$ are constructed based on α_{bt} and β_{kt}, respectively. For instance, if $\alpha_{bt}=1$, then $(b,t)\in\mathcal{M}$, otherwise, $(b,t)\notin\mathcal{M}$. The many-to-many matching problem can be solved via swap [35]. Consider a set $\mathcal{M}_1$, where $(b,t)\in\mathcal{M}_1$ but $(b',t')\notin\mathcal{M}_1$. We define a swap $\mathcal{S}_{b't'}^{bt}$ as the operation of converting $\mathcal{M}_1$ into $\mathcal{M}_2$ by removing (b,t) and adding (b',t'), i.e., setting $\alpha_{bt}=0$ and $\alpha_{b't'}=1$. A swap happens if $\mathcal{M}_1$ and $\mathcal{M}_2$ meet the following conditions:

$$1.\ \mathcal{M}_2 \text{ satisfies constraints (5c) and (5g);} \tag{13}$$

$$2.\ y(\mathcal{M}_1,\mathcal{N})>y(\mathcal{M}_2,\mathcal{N}). \tag{14}$$

Define $\mathfrak{S}$ as the set containing all the possible $\mathcal{S}_{b't'}^{bt}$.

Analogous to beam-to-timeslot swap, we consider a set $\mathcal{N}_1$, where $(k,t)\in\mathcal{N}_1$ but $(k',t')\notin\mathcal{N}_1$. Define a swap $\bar{\mathcal{S}}_{k't'}^{kt}$ as the operation of converting $\mathcal{N}_1$ into $\mathcal{N}_2$ by removing (k,t) and introducing (k',t'), i.e., setting $\beta_{kt}=0$ and $\beta_{k't'}=1$. A swap occurs if $\mathcal{N}_1$ and $\mathcal{N}_2$ satisfy the following conditions:

$$1.\ \mathcal{N}_2 \text{ satisfies constraints (5d);} \tag{15}$$

$$2.\ k,k'\in\mathcal{K}_b \text{ and } \alpha_{bt}=\alpha_{bt'}=1; \tag{16}$$

$$3.\ y(\mathcal{M},\mathcal{N}_1)>y(\mathcal{M},\mathcal{N}_2). \tag{17}$$

Define $\bar{\mathfrak{S}}$ as the set containing all the possible $\bar{\mathcal{S}}_{k't'}^{kt}$.

We summarize the procedure of UBA in Alg. 2. Denote N' as the maximum number of iterations. Line 3 to line 13 represent the swap of beam-to-timeslot matching and line 14 to line 22 indicate the terminal-to-timeslot swap. Remark that the algorithm starts to assign terminals to timeslots once beam-to-timeslot swap is executed. The algorithm terminates when the number of iterations reaches N', there is no more valid swap, or all the terminals are satisfied with demand.

In UBA, the complexity for each iteration consists of two parts, i.e., beam-to-timeslot swap and terminal-to-timeslot swap. The numbers of all the possible beam-to-timeslot and terminal-to-timeslot swaps are at most $TB_0\times T(B-B_0)$ and $B_0\times TK_0\times T(K'-K_0)$, respectively. For each iteration, the worst case is to optimize power for all the swaps in $\mathfrak{S}$ and $\bar{\mathfrak{S}}$ by Alg. 1. Thus the complexity of UBA is $\mathcal{O}(N'T^2B_0(B-B_0+K_0(K'-K_0))\max\{N\psi\log(\frac{1}{\varepsilon}),\varrho^{-2}\})$. Remark that, in practice, the complexity can be largely reduced by eliminating a certain number of swaps that do not satisfy conditions (13), (15), and (16).

Algorithm 2 UBA

Input: Feasible $\tilde{p}_{kt}$, $\tilde{\alpha}_{bt}$, and $\tilde{\beta}_{kt}$ (corresponding to $\tilde{\mathcal{M}}$ and $\tilde{\mathcal{N}}$).

1: **repeat**
2: Construct $\mathfrak{S}$ based on $\tilde{\alpha}_{bt}$ and (13).
3: **if** $\mathfrak{S}\neq\varnothing$ **then**
4: Select a swap $\mathcal{S}_{b't'}^{bt}$ and construct $\mathcal{M}$ with (b',t').
5: Optimize p_{kt} under $\mathcal{M}$ via Alg. 1.
6: **else**
7: UBA terminates.
8: **end if**
9: **if** $\tilde{\mathcal{M}}$ and $\mathcal{M}$ do not satisfy (14) **then**
10: Remove $\mathcal{S}_{b't'}^{bt}$ from $\mathfrak{S}$.
11: Move to line 3.
12: **end if**
13: Let $\tilde{\mathcal{M}}=\mathcal{M}$ and $\tilde{p}_{kt}=p_{kt}$ and update $\tilde{\alpha}_{bt}$, $\tilde{\beta}_{kt}$, and $\tilde{\mathcal{N}}$. Construct $\bar{\mathfrak{S}}$ based on $\tilde{\beta}_{kt}$, (15), and (16).
14: **if** $\bar{\mathfrak{S}}\neq\varnothing$ **then**
15: Select a swap $\bar{\mathcal{S}}_{k't'}^{kt}$ and construct $\mathcal{N}$ with (k',t').
16: Optimize p_{kt} under $\mathcal{N}$ via Alg. 1.
17: **end if**
18: **if** $\tilde{\mathcal{N}}$ and $\mathcal{N}$ do not satisfy (17) **then**
19: Remove $\bar{\mathcal{S}}_{k't'}^{kt}$ from $\bar{\mathfrak{S}}$.
20: Move to line 14.
21: **end if**
22: Let $\tilde{\mathcal{N}}=\mathcal{N}$ and $\tilde{p}_{kt}=p_{kt}$ and update $\tilde{\beta}_{kt}$.
23: **until** the number of iterations reaches N' or $R_k=D_k$ $\forall k\in\mathcal{K}$

Output: $\tilde{p}_{kt}$, $\tilde{\alpha}_{bt}$, $\tilde{\beta}_{kt}$.

V. An MICP Approximation Approach for Lower Bound

In this section, we resolve $\mathcal{P}_0$'s non-convexity by intentionally simplifying the inter-beam interference, and construct an MICP formulation to enable a lower bound for $\mathcal{P}_0$. We observe that, in some BH cases, the inter-beam interference may become negligible, e.g., illuminating two distant beams. If this interference can be ignored, $\mathcal{P}_0$ becomes an MICP problem. In this case, p_{kt} for terminals in $\mathcal{K}_b$ can be derived as follows,

$$\begin{aligned}
p_{1t} &= \left(2^{\frac{R_{1t}}{W}}-1\right)\frac{\sigma^2}{|h_{b1}|^2},\\
p_{2t} &= \left(2^{\frac{R_{2t}}{W}}-1\right)\left(p_{1t}+\frac{\sigma^2}{|h_{b2}|^2}\right),\\
&\cdots\\
p_{K_bt} &= \left(2^{\frac{R_{K_bt}}{W}}-1\right)\left(\sum_{k'=1}^{K_b-1}p_{k't}+\frac{\sigma^2}{|h_{bK_b}|^2}\right).
\end{aligned} \tag{18}$$

Thus (5b) can be rewritten in an equivalent expression as,

$$\sum_{k=1}^{K_b}\left(\frac{\sigma^2}{|h_{bk}|^2}-\frac{\sigma^2}{|h_{b(k-1)}|^2}\right)2^{\frac{\sum_{k'=k}^{K_b}R_{k't}}{W}}-\frac{\sigma^2}{|h_{bK_b}|^2}\le P,\quad \forall b\in\mathcal{B},\quad \forall t\in\mathcal{T}, \tag{19}$$

where we define that $\frac{\sigma^2}{|h_{b0}|^2}=0$. Then $\mathcal{P}_0$ becomes,

$$\mathcal{P}_3: \quad \min_{\alpha_{bt},\beta_{kt},R_{kt},\delta_k} \sum_{k\in\mathcal{K}} \delta_k^2 \tag{20a}$$

$$\text{s.t. } (19),(5c),(5d),(5f),(5g),(7c), \tag{20b}$$

$$R_{kt} \le R^{\max}\beta_{kt}, \quad \forall k\in\mathcal{K},\ \forall t\in\mathcal{T}, \tag{20c}$$

where $R^{\max}$ is a constant, no smaller than all possible R_{kt}. Constraints (20c) connect R-variables with β-variables, where $R_{kt}=0$ if $\beta_{kt}=0$, otherwise, $R_{kt}\le R^{\max}$. $\mathcal{P}_3$ is an MICP with the presence of exponential cones in (19) and the quadratic cones in (20a). The optimum of $\mathcal{P}_3$ can be achieved by branch-and-bound or outer approximation approach [34].

Note that, since inter-beam interference has been intentionally removed, the optimum of $\mathcal{P}_3$ is no larger than that of $\mathcal{P}_0$ and thus can be viewed as a lower bound of $\mathcal{P}_0$.

Remark 1: The gap between the lower bound (the optimum of $\mathcal{P}_3$) and the optimum of $\mathcal{P}_0$ follows three cases:

- Zero gap: The optimum at $\mathcal{P}_0$ and $\mathcal{P}_3$ is equivalent if only one beam is illuminated at each timeslot since there is no inter-beam interference in the system.
- Close-to-zero gap: $\mathcal{P}_3$ provides a close lower bound to the optimum of $\mathcal{P}_0$ if the level of inter-beam interference keeps low.
- Large gap: In some cases, the lower bound becomes loose when inter-beam interference is strong. However, due to the inherent characteristics in BH optimization, only the beams with less mutual interference are preferred to be activated at the same timeslot. Thus, this undesired issue can be avoided in a majority of cases. □

VI. An Efficient Algorithm for Joint Optimization

UBA aims at providing a tight upper bound (or near-optimal solution) to $\mathcal{P}_0$ at the expense of high complexity. To further reduce the computational complexity, we design a low-complexity approach, i.e., E-JPBT, to provide an efficient solution for $\mathcal{P}_0$. The basic idea of E-JPBT is to divide the whole decision process of $\mathcal{P}_0$ into T stages (or timeslots) and then solve a subproblem at each stage or timeslot. To avoid directly tackling integer variables with large complexity, the subproblem for each timeslot is relaxed to a continuous problem, which can be solved by Alg. 1.

The residual demand for terminal k before timeslot t is,

$$\bar{D}_{kt}=\begin{cases} D_k-\sum_{\tau=1}^{t-1}R_{k\tau}, & \text{if } t>1,\\ D_k, & \text{if } t=1. \end{cases} \tag{21}$$

At the t-th timeslot, the resource allocation problem for the current timeslot is expressed as,

$$\mathcal{P}_0(t): \quad \min_{\alpha_{bt},\beta_{kt},p_{kt}} \sum_{k\in\mathcal{K}}\left(R_{kt}-\bar{D}_{kt}\right)^2 + \sum_{k\in\mathcal{K}}\phi_k\left[R_k^{\min}-R_{kt}-\sum_{\tau=0}^{t-1}R_{k\tau}\right]^+ \tag{22a}$$

$$\text{s.t. } \sum_{k\in\mathcal{K}_b} p_{kt}\le 1, \quad \forall b\in\mathcal{B}, \tag{22b}$$

Algorithm 3 E-JPBT

Input: ϕ_k.

1: **for** $t=1,\dots,T$ **do**
2: Optimize $\bar{\alpha}_{bt}$ and $\bar{\beta}_{kt}$ by solving $\mathcal{P}_4(t)$ via Alg. 1.
3: Select $j^*=\arg\max_j\{\sum_{b\in\mathcal{B}_j}\bar{\alpha}_{bt}\}$.
4: Set $\alpha_{bt}=1, \forall b\in\mathcal{B}_{j^*}$.
5: Select K_0 largest-$\bar{\beta}_{kt}$ terminals for each illuminated beam.
6: Set accordingly $\beta_{kt}=1$.
7: Optimize p_{kt} by solving $\mathcal{P}_4(t)$ via Alg. 1 with α_{bt} and β_{kt}.
8: Calculate $\bar{D}_{kt}$ by (21).
9: **end for**
10: Optimize p_{kt} via Alg. 1 with determined α_{bt} and β_{kt}.

Output: α_{bt}, β_{kt}, and p_{kt}.

$$\sum_{b\in\mathcal{B}}\alpha_{bt}\le B_0, \tag{22c}$$

$$\sum_{k\in\mathcal{K}_b}\beta_{kt}\le K_0\alpha_{bt}, \quad \forall b\in\mathcal{B}, \tag{22d}$$

$$p_{kt}\le\beta_{kt}, \quad \forall k\in\mathcal{K}_b, \tag{22e}$$

$$\alpha_{bt}+\alpha_{b't}\le 1, b\ne b', \quad \forall (b,b')\in\Omega, \tag{22f}$$

where the second term of the objective is the penalty for constraints (5f) and $\phi_k>0$ is the penalty factor. The objective is penalized if the rate of terminal k is lower than $R_k^{\min}$, which means more resources should be allocated to this terminal in the later timeslots.

Since $\mathcal{P}_0(t)$ is MINCP and is still challenging, we relax α_{bt} and β_{kt} into continuous variables, i.e., $0\le\bar{\alpha}_{bt}\le 1$ and $0\le\bar{\beta}_{kt}\le 1$. Then we convert the R-function into $f_{kt}^R(\theta_{kt},p_{kt})$ as expressed in (9) via quadratic transform. $\mathcal{P}_0(t)$ can be reformulated as,

$$\mathcal{P}_4(t): \quad \min_{\bar{\alpha}_{bt},\bar{\beta}_{kt},p_{kt},\theta_{kt}} \sum_{k\in\mathcal{K}}\left(f_{kt}^R-\bar{D}_{kt}\right)^2 + \sum_{k\in\mathcal{K}}\phi_k\left[R_k^{\min}-f_{kt}^R-\sum_{\tau=0}^{t-1}f_{k\tau}^R\right]^+ \tag{23a}$$

$$\text{s.t. } (22b),(22c),(22d),(22e),(22f), \tag{23b}$$

which can be solved via Alg. 1. We define $\mathcal{B}_j\subseteq\mathcal{B}$ as the j-th beam group. Note that the beam groups are constructed based on Ω. We schedule the beam group on the basis of $j^*=\arg\max_j\{\sum_{b\in\mathcal{B}_j}\bar{\alpha}_{bt}\}$. Then we select K_0 largest-$\bar{\beta}_{kt}$ terminals for each active beam. Accordingly, we decide α_{bt} and β_{kt} for the current timeslot. To update the residual demand $\bar{D}_{kt}$, we solve the remaining of $\mathcal{P}_4(t)$ via Alg. 1 with the decided integer solution. At the end, with all determined α_{bt} and β_{kt}, we optimize p_{kt} by solving $\mathcal{P}_1$ via Alg. 1.

The procedure of E-JPBT is summarized in Alg. 3, where line 2 to line 6 are the process of determining integer variables for each timeslot. In line 2, we solve the relaxed problem via Alg. 1 and obtain the continuous solution, $\bar{\alpha}_{bt}$ and $\bar{\beta}_{kt}$. The decisions of α_{bt} and β_{kt} are described in line 4 and

TABLE I
SIMULATION PARAMETERS

Parameter	Value
Frequency, f^{fr}	20 GHz (Ka band)
Bandwidth, W	500 MHz
Satellite location	13° E
Satellite height	35,786 km
Beam radiation pattern	Provided by ESA [23]
Power budget per beam, P	20 dBW
Receive antenna gain, G_k^{rx}	42.1 dBi
Noise power, σ^2	-126.47 dBW
Number of timeslots, T	256
Number of beams, B	37
Maximum active beams, B_0	5
Number of terminals per beam, K'	5
Minimum capacity, $R_k^{\min}$	5 Mbps
Traffic demand, D_k	100 Mbps to 1.2Gbps
Error ratio of imperfect SIC	10^{-4}
Maximum multiplexed terminals, K_0	3
Maximum iterations in Alg. 1, N	20
Maximum iterations in Alg. 2, N'	100

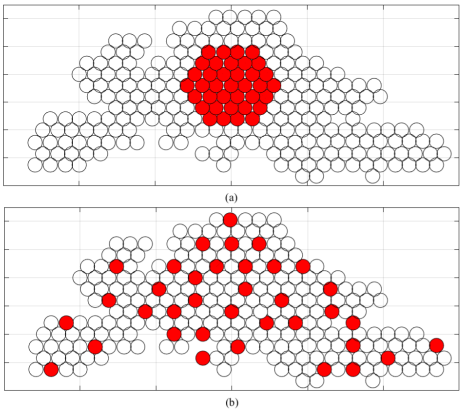


Fig. 2. Beam pattern covering Europe provided by ESA [23] and the adopted two scenarios, where BH is operated among the considered 37 beams (highlighted in red color).

line 6, respectively. With determined integer variables, power optimization is executed via Alg. 1 to calculate $\bar{D}_{kt}$. At the end of E-JPBT, we optimize power with all the determined integer solution in line 7. In conclusion, E-JPBT needs to apply Alg. 1 for $2T+1$ times, and thus the complexity of E-JPBT is $\mathcal{O}((2T+1)\max\{N\psi\log(\frac{1}{\varepsilon}), \varrho^{-2}\})$.

VII. PERFORMANCE EVALUATION

A. Simulation Settings and Benchmarks

In this section, we evaluate the performance of the proposed NOMA-BH scheme and the proposed algorithms in a multi-beam satellite system. The parameter settings are summarized in Table I unless stated otherwise. The beam radiation pattern is provided by European Space Agency (ESA) [23], which is depicted in Fig. 2. We set $T = 256$, which is larger than the minimum required number of timeslots, $\left\lceil \frac{K'}{K_0} \right\rceil \left\lceil \frac{B}{B_0} \right\rceil = 16$. In this setting, all the terminals can be scheduled to at least one timeslot. The results are averaged by 1000 instances. In NOMA, we consider a practical issue in performance evaluation, i.e., residual interference in decoding terminals' signals due to imperfect SIC [36]. Note that imperfect SIC is always considered in performance evaluation. When calculating the offered-requested data rate gap, the units of capacity and demand are unified as Mbps.

TABLE II
POWER CONSUMPTION (IN WATTS) OF DIFFERENT SCHEMES IN FIG. 3

UBA	E-JPBT	BH-OMA	1c-NOMA	2c-NOMA	4c-NOMA
227.0	221.5	192.8	860.44	584.45	929.24

In simulation, we aim to demonstrate the applicability of the proposed BH-NOMA schemes in various satellite scenarios. We consider two typical satellite scenarios [1] (highlighted in Fig. 2):

- Scenario 1 (Fig. 2(a)): Within a concentrated area, we extract a set of adjacent beams from 245 beams. Scenario 1 provides a harsh scenario to evaluate the BH-NOMA schemes, aiming at investigating how to manage inter-beam interference among the illuminated beams with relatively short distance than that in Scneario 2.
- Scenario 2 (Fig. 2(b)): We randomly select a set of non-adjacent beams from 245 beams, where BH is performed within a large area. One instance is to serve terminals in some distributed target areas, e.g., mountains or rural areas. Since no adjacent beams exist in Scenario 2, the inter-beam interference is typically smaller than that in Scenario 1.

We summarize the benchmark schemes as the following for different purposes of performance evaluation. To investigate the benefits of combining BH and NOMA, we compare the proposed BH-NOMA schemes with the following standalone schemes either considering BH or NOMA (referring to Fig. 3 and Table II):

- BH-OMA (without NOMA): The BH-OMA problem can be formulated by simply restricting only one terminal at each timeslot, i.e., $K_0 = 1$ in $\mathcal{P}_0$, and then apply Alg. 2 to obtain the optimized result.
- 1c-NOMA (without BH): NOMA is adopted with 1-color frequency-reuse pattern (full-frequency reuse). All the beams keep illuminated without considering BH.
- 2c-NOMA (without BH): NOMA is coordinated with 2-color frequency-reuse pattern where each color represents either vertical and horizontal polarization such that adjacent two beams can occupy orthogonal resources.
- 4c-NOMA (without BH): NOMA is coordinated with 4-color frequency-reuse pattern. In the system, the frequency band is equally divided into two segments and each segment utilizes vertical and horizontal polarization. In this way, the adjacent four beams can occupy four different colors and the inter-beam interference can be reduced.

We also compare the performance achieved by the proposed algorithms with the following benchmarking schemes from the literature (referring to Fig. 5):

- RA: We apply the resource allocation scheme proposed in [37] to determine the number of scheduled timeslots for each beam. Then Alg. 3 is applied to decide terminal-timeslot assignment and power allocation.

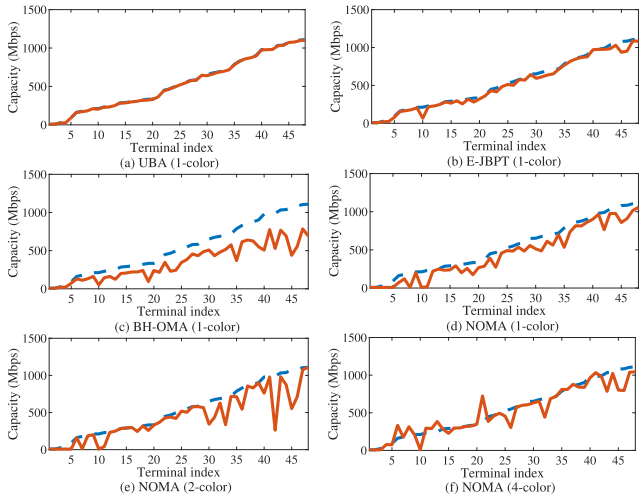


Fig. 3. An illustration of gaps between each user's data demand (blue dashed line) and the offered capacity (red solid line) ($K = 48$, $B = 16$, $B_0 = 4$, and $K_0 = 2$).

- MaxSINR: An approach proposed in [7] and [12] is adopted to determine the illuminated beams at each timeslot by selecting the beams with maximum SINR. Then Alg. 3 is then adapted to optimize power allocation and terminal-timeslot assignment.
- MinCCI: An efficient approach used in [12] is applied to activate beams with the minimum inter-beam interference, then Alg. 3 is adopted analogously to MaxSINR.

For a fair comparison with other metrics for evaluating the offered-requested data rate matching, we adapt UBA to optimize the following widely-used objective functions (referring to Table III):

- Scheme 1: The objective is to max-min offered-capacity-to-requested-traffic ratio (OCTR), i.e., $\max \min_{k\in\mathcal{K}} \frac{R_k}{D_k}$, [3], [6], [18] such that the worst capacity-demand mismatch effects among terminals can be mitigated.
- Scheme 2: The objective aims at minimizing the total unmet capacity of terminals, i.e., $\min \sum_{k\in\mathcal{K}} [D_k - R_k]^+$, [3], [22], [38].

B. Benefits of Jointly Considering BH and NOMA

In Fig. 3, we discuss the benefits and evaluate the performance gains of combining BH and NOMA. The proposed BH-NOMA schemes, i.e., UBA and E-JPBT, are compared with the standalone schemes, either considering BH or NOMA. We adopt 1-color frequency-reuse pattern in UBA, E-JPBT, and BH-OMA. The gaps are large in standalone NOMA or BH schemes, i.e., Fig. 3(c) to Fig. 3(f). In contrast, by jointly optimizing BH and NOMA, the proposed BH-NOMA schemes in Fig. 3(a) and Fig. 3(b) significantly alleviate the mismatch effects, e.g., the objective value is reduced from $10^5 - 10^8$ in (Fig. 3(c) – Fig. 3(f)) to $10^2 - 10^3$ (in Fig. 3(a) and Fig. 3(b)). In Table II, we further summarize the power consumption in these schemes. BH-OMA consumes the least power, slightly lower than UBA and E-JPBT, but does not perform well in capacity-demand matching.

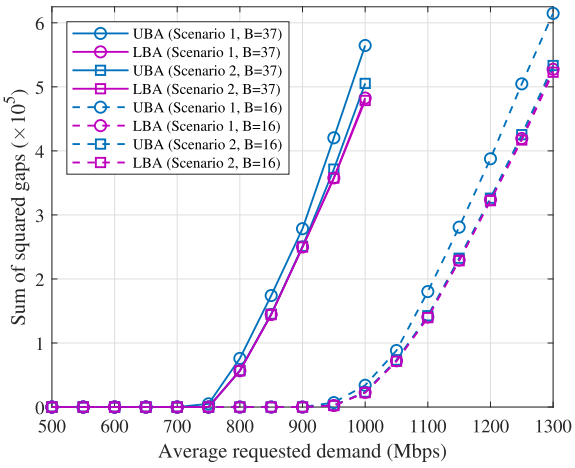


Fig. 4. The gap performance between upper bound and lower bound, where we set 5 terminals in each beam and $K_0 = 3$.

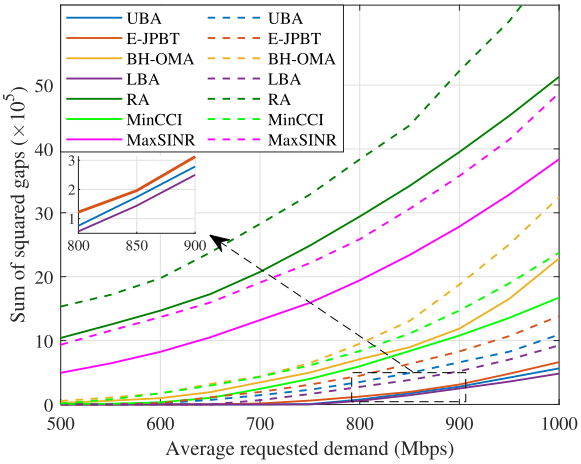


Fig. 5. The gap performance with respect to traffic demand among the proposed schemes and benchmarks. (Scenario 1, 5 terminals per beam, $K_0 = 3$) (Solid line: under free-space channel model [3], [6], [10]; Dash line: atmospheric channel model with long-term effects and rain effects [40]).

Compared to 1c-NOMA, 2c-NOMA, and 4c-NOMA, the proposed UBA and E-JPBT, by augmenting both power- and time-domain flexibilities, consume much less power and achieve good trade-offs between power saving and capacity-demand mismatch reduction.

C. Performance in Bounding and Approaching the Optimum

We evaluate the tightness of upper and lower bounds in Scenario 1 and Scenario 2 with 16 or 37 beams. From Fig. 4, we observe that the bounding gap increases as the average demand grows. For presentation convenience, we apply the term "$\times 10^5$" in y-label as the magnitude of the values on y-axis. The proposed bounding scheme achieves near-zero gaps in Scenario 2, even for the cases with large demand. This is because the inter-beam interference can maintain at a very low level when distant beams are activated. When this small amount of inter-beam interference is intentionally neglected in LBA, it has limited impact and therefore keeps a tight lower bound for the optimum. In contrast, when Scenario 1 is considered, a larger amount of inter-beam interference is removed in LBA, thus results in larger gaps, e.g., 14.9% in

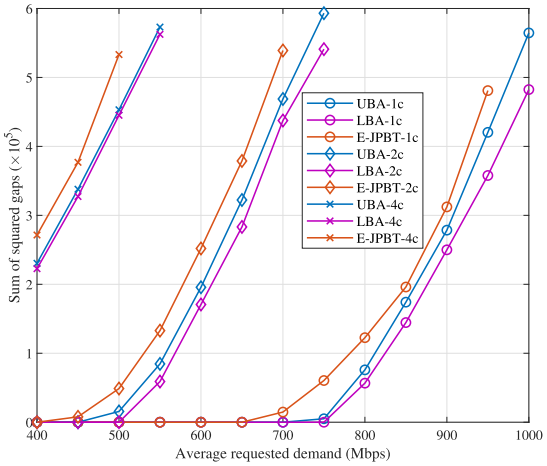


Fig. 6. The gap performance value with respect to traffic demand of the proposed BH-NOMA schemes in different scenarios with 1-color, 2-color, adn 4-color frequency-reuse patterns.

TABLE III
THE PERFORMANCE COMPARISON AMONG DIFFERENT METRICS

Metrics \ Schemes	UBA	Scheme 1	Scheme 2
Sum of squared gaps $\sum_{k\in\mathcal{K}}(R_k - D_k)^2$	1.57×10^3	3.0×10^4	1.69×10^4
The worst OCTR	0.93	0.96	0.88
Sum unmet capacity $\sum_{k\in\mathcal{K}}[D_k - R_k]^+$	218.47	1013.181	215.30

37 beams and 19.2% in 16 beams. The numerical results are consistent with the analysis in Remark 1. By our design in LBA, less interference is neglected and a tighter lower bound can be obtained. We can observe three major differences of the optimized BH solutions between Fig. 2(a) and Fig. 2(b). Firstly, the optimized BH solutions lead to smaller capacity-demand gaps, i.e., objective value, in Scenario 2 than that in Scenario 1. Secondly, in Scenario 1, the optimized BH scheme may prefer to activate a fewer number of beams per timeslot due to the presence of higher-level inter-beam interference, while more beams tend to be activated together in Scenario 2 due to the fact of distantly located beams with less mutual interference. Thirdly, the activated beams are typically non-neighboring and far away from each other in order to avoid strong inter-beam interference in Scenario 1, which may not always be the case in the optimized BH solutions of Scenario 2. This is because a beam can possibly be activated together with its nearest or neighboring beams (but geographically non-adjacent in Scenario 2) at the optimum when the interference maintains at the low level.

D. Performance Comparison Between the Proposed Algorithms and Benchmarks

In Fig. 5, we compare the performance of the proposed UBA, LBA, and E-JPBT with BH-OMA and benchmarking schemes from the literature. We observe that the proposed schemes outperform all the four benchmarks in reducing the gap between requested and offered data rates. Firstly, due to the higher spectral efficiency in NOMA, the proposed BH-NOMA schemes outperform BH-OMA, e.g., 80.8% and

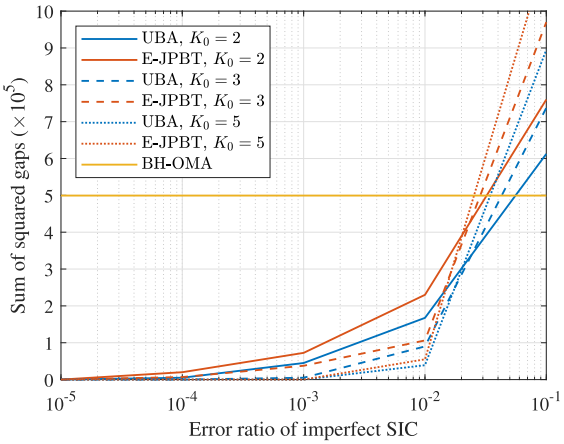


Fig. 7. The gap performance versus error ratio of imperfect SIC of the proposed NOMA schemes.

76.3% improvement in UBA and E-JPBT. Compared to RA, MaxSINR, and MinCCI, E-JPBT decreases the effect of offered-requested data mismatches by 93.2%, 90.7%, 70.4%, respectively. The proposed BH-NOMA schemes can largely reduce the mismatch effects by joint optimization of BH and NOMA compared to GA, MaxSINR, and MinCCI. We also observe that E-JPBT can achieve the cost close to the upper bound with a gap of 18.95%. Moreover, we evaluate the schemes under the channel model with atmospheric fading including long-term effects and rain effects [40]. The results verify that the advantages of the proposed UBA and E-JBPT over other benchmarks remain. The two schemes can achieve good performance in reducing the capacity-demand gaps under different channel models. The average computational time of UBA, E-JPBT, MinCCI, and MaxSINR normalized by that of RA is 14.16, 1.15, 1.10, and 1.08, respectively, where E-JPBT consumes 91.88% less time compared to UBA and maintains the same magnitude of computational time with other efficient benchmark schemes. Considering the observed performance gains, E-JPBT thus achieves a good trade-off between complexity and performance compared to other schemes.

E. The Performance of the Proposed Schemes With Different Frequency-Reuse Patterns

In Fig. 6, we evaluate the applicability of the proposed BH-NOMA schemes in the scenarios with the implementation of 1-color, 2-color, and 4-color frequency-reuse patterns. The performance of the proposed schemes in all the three scenarios is promising. With higher spectral efficiency, the proposed schemes in 1-color scenario can perfectly match capacity to demand when the requested demand is no larger than 650 Mbps. With less inter-beam interference, the average performance gaps between upper bound and lower bound in 2-color and 4-color scenarios are 11.23% and 2.32%, respectively, which are smaller than that in 1-color scenario. The result also verifies the conclusion in Remark 1.

F. Comparison Among Different Metrics for Evaluating the Offered-Requested Data Rate Mismatch

Next, we compare the offered-requested data mismatch performance among different metrics. In Table III,

we summarize the performance, where each scheme is solved by its own objective, e.g., 1.57×10^3 is obtained by UBA with the objective (5a) in the first row. By summarizing the obtained solutions, the results for the other two metrics can be obtained, e.g., the worst OCTR for UBA in the second row. As expected, all the three schemes perform the best with their own objectives, referring to the diagonal values, but can degrade sharply when measured with other metrics. The proposed BH-NOMA scheme shows good adaptation and generalization capabilities among different metrics, which means that UBA achieves the best performance in reducing the sum of squared gaps, and slightly losses around 1% to 3% performance in max-min OCTR and reducing unmet capacity than the other two schemes.

G. Impact of Imperfect SIC on BH-NOMA Performance

At last, we evaluate the impact of practical issues of NOMA on the performance of UBA and E-JPBT. We introduce $0 \leq \eta_k \leq 1$ to represent residual interference due to imperfect SIC [36]. Specifically, the intra-beam interference in (1) is rewritten as,

$$\sum_{\substack{k' \in \mathcal{K}_b \setminus \{k\} \\ k' < k}} |h_{bk}|^2 p_{k't} + \sum_{\substack{k' \in \mathcal{K}_b \setminus \{k\} \\ k' > k}} |h_{bk}|^2 p_{k't} \eta_k. \tag{24}$$

The result in Fig. 7 shows the applicability of the proposed BH-NOMA schemes to imperfect-SIC scenarios. We can observe that the performance increases slowly when the error ratio of imperfect SIC is small, e.g., from 10^{-5} to 10^{-2}. When the ratio increases more than 10^{-2}, OMA might become a better choice. Besides, when the error is large, e.g., 10^{-1}, the mismatch effect in the case of $K_0 = 5$ is worse than those of $K_0 = 2$ and $K_0 = 3$. This is because the intra-beam interference caused by imperfect SIC increases with the number of co-channel terminals in the same beam.

VIII. Conclusion

In this paper, we have investigated joint resource optimization for the coexisted BH-NOMA systems. A resource allocation problem has been formulated to minimize the gap between requested and offered data rates of terminals by jointly optimizing power allocation, beam scheduling, and terminal-timeslot assignment. We have identified the NP-hardness of the problem and proposed an effective bounding scheme, UBA and LBA, to benchmark the optimality. To reduce computational complexity, we have designed an efficient algorithm for joint optimization. In the end, we have verified the benefits of combining BH and NOMA, and demonstrated the advantages of the proposed BH-NOMA schemes compared to different benchmarks.

Appendix A
Proof of Lemma 1

Proof: We construct a polynomial-time reduction from three-dimensional matching (3DM) problem [39], one of the typical NP-complete problems, to an instance of the decision-version problem of $\mathcal{P}_0$. Consider three different sets $\mathcal{X}$, $\mathcal{Y}$, and $\mathcal{Z}$, where $|\mathcal{X}| = |\mathcal{Y}| = |\mathcal{Z}|$. The 3DM problem is to check whether there exists a matching set $\Theta \subset \mathcal{X} \times \mathcal{Y} \times \mathcal{Z}$ such that $x_1 \neq x_2$, $y_1 \neq y_2$, and $z_1 \neq z_2$ for any two different triplets (x_1, y_1, z_1) and (x_2, y_2, z_2) in Θ. If yes, Θ is called a 3DM.

Consider a special case with one terminal per beam, i.e., $K = B$. In this case, we use terminals' indexes and beams' interchangeably. The set of beams is divided into two subsets, $\mathcal{B}_1$ and $\mathcal{B}_2$, where $\mathcal{B}_1 \cap \mathcal{B}_2 = \varnothing$, $\mathcal{B}_1 \cup \mathcal{B}_2 = \mathcal{B}$, and $|\mathcal{B}_1| = |\mathcal{B}_2| = \frac{B}{2}$. For any beam $b \in \mathcal{B}_i$, $\forall i = \{1, 2\}$, the channel gains satisfy the following conditions,

$$|h_{b'b}|^2 = \begin{cases} 1 + \epsilon, & \text{if } b' = b, \\ 1 + \dfrac{\epsilon}{2}, & \text{else if } b' \in \mathcal{B}_i, \\ \epsilon, & \text{else if } b' \in \mathcal{B}_j, j \neq i, \end{cases} \tag{26}$$

where $0 < \epsilon \leq 2^{\frac{1}{B}} - 1$. We set the parameters as follows: $P = 1$, $\sigma^2 = \epsilon$, $B_0 = 2$, $T = \frac{B}{2}$, $\Omega = \varnothing$, $R_b^{\min} = 1$, and $D_b \gg 1$.

First, we prove that the instance problem is feasible if the answer to the 3DM problem is yes. We let $\mathcal{X} = \mathcal{T}$, $\mathcal{Y} = \mathcal{B}_1$, and $\mathcal{Z} = \mathcal{B}_2$. For any two triplets (t_1, b_1, b'_1) and (t_2, b_2, b'_2) in Θ, the following relationships hold: $t_1 \neq t_2$, $b_1 \neq b_2$, and $b'_1 \neq b'_2$. In this case, any two beams scheduled to the same timeslot are from different subsets. If beam b is illuminated at timeslot t, the rate of each beam is derived as $\log_2(1 + \frac{|h_{bb}|^2 P}{|h_{b'b}|^2 P + \sigma^2}) = \log_2(1 + \frac{1+\epsilon}{\epsilon+\epsilon}) > 1 = R_b^{\min}$, which meets constraints (5b) to (5g). Thus the instance problem is feasible.

Next, we prove that if the instance problem is feasible, the answer to the 3DM problem is yes. Since $T = \frac{B}{2}$ and $B_0 = 2$, all beams are scheduled only once. If there exist two beams from the same subset scheduled to the same timeslot, then the rates for these two beams are $\log_2(1 + \frac{|h_{bb}|^2 P}{|h_{b'b}|^2 P + \sigma^2}) = \log_2(1 + \frac{1+\epsilon}{1+\frac{\epsilon}{2}+\epsilon}) < \log_2(1+1) = 1 = R_b^{\min}$, which violates the minimum-rate constraint in (5f). To meet the constraints, the interference must be ϵ, requiring that any two beams scheduled to the same timeslot are from different subsets. Thus, the answer to the 3DM problem is yes. In conclusion, the yes answer to the 3DM problem is the necessary and sufficient condition of the existence of a feasible solution of the instance problem. As the 3DM problem is NP-complete, the Lemma follows. □

Appendix B
Proof of Proposition 1

Proof: The proposition can be proven by raising the contradiction that there exist some terminals with $R_k > D_k$ at the optimum. Define $\mathcal{K}_t$ as the set of the terminals scheduled to the t-th timeslot. We divide $\mathcal{K}_t$ into two subsets, $\mathcal{K}_t^+$ and $\mathcal{K}_t^-$, containing terminals with $R_k > D_k$ and $R_k \leq D_k$, respectively. Let p_{kt}^* be the optimal power. For presentation convenience, we denote $I_{k'kt}$ as the interference of terminal k caused by k' at timeslot t. We apply $0 < \zeta \leq 1$ to adjust the power of all the terminals in $\mathcal{K}_t^+$. As p_{kt}^* is optimal, $\zeta = 1$ should be optimal. For $k \in \mathcal{K}_t^+$, the SINR is expressed

$$\tilde{f}'(\zeta; p_{kt}^*) = \sum_{k\in\mathcal{K}_t^+} \frac{\frac{2(R_k-D_k)\gamma_{kt}}{\zeta(1+\gamma_{kt})}\left(\sum\limits_{k'\in\mathcal{K}_t^-} I_{k'kt}+\sigma^2\right)}{\sum\limits_{k'\in\mathcal{K}_t^+\setminus\{k\}}\zeta I_{k'kt}+\sum\limits_{k'\in\mathcal{K}_t^-} I_{k'kt}+\sigma^2} - \sum_{k\in\mathcal{K}_t^-} \frac{\frac{2(R_k-D_k)\gamma_{kt}}{\zeta(1+\gamma_{kt})}\sum\limits_{k'\in\mathcal{K}_t^+} I_{k'kt}}{\sum\limits_{k'\in\mathcal{K}_t^+}\zeta I_{k'kt}+\sum\limits_{k'\in\mathcal{K}_t^-\setminus\{k\}} I_{k'kt}+\sigma^2} \tag{25}$$

as,

$$\gamma_{kt} = \frac{|h_{bk}|^2\zeta p_{kt}^*}{\sum_{k'\in\mathcal{K}_t^+\setminus\{k\}}\zeta I_{k'kt}+\sum_{k'\in\mathcal{K}_t^-} I_{k'kt}+\sigma^2}. \tag{27}$$

The SINR of terminals in $\mathcal{K}_t^-$ is,

$$\gamma_{kt} = \frac{|h_{bk}|^2 p_{kt}^*}{\sum_{k'\in\mathcal{K}_t^+}\zeta I_{k'kt}+\sum_{k'\in\mathcal{K}_t^-\setminus\{k\}} I_{k'kt}+\sigma^2}. \tag{28}$$

Given p_{kt}^*, the objective can be viewed as the function of ζ, say $\tilde{f}(\zeta; p_{kt}^*)$. We present the derivative of $\tilde{f}(\zeta; p_{kt}^*)$ in (25), shown at the top of the page, which is obviously larger than zero since $R_k > D_k$ for terminals in $\mathcal{K}_t^+$ and $R_k < D_k$ for terminals in $\mathcal{K}_t^-$. Thus the objective can be smaller by letting $\zeta < 1$ to reduce power of the terminals in $\mathcal{K}_t^+$, which contradicts the assumption of the optimality. Thus the proposition. □

REFERENCES

[1] G. Maral, M. Bousquet, and Z. Sun, *Satellite Communications Systems: Systems, Techniques and Technology*. Hoboken, NJ, USA: Wiley, 2020.

[2] O. Kodheli, "Satellite communications in the new space era: A survey and future challenges," *IEEE Commun. Surveys Tuts.*, vol. 23, no. 1, pp. 70–109, 4th Quart., 2021.

[3] G. Cocco, T. De Cola, M. Angelone, Z. Katona, and S. Erl, "Radio resource management optimization of flexible satellite payloads for DVB-S2 systems," *IEEE Trans. Broadcast.*, vol. 64, no. 2, pp. 266–280, Jun. 2018.

[4] P. Angeletti, D. Fernandez Prim, and R. Rinaldo, "Beam hopping in multi-beam broadband satellite systems: System performance and payload architecture analysis," in *Proc. 24th AIAA Int. Commun. Satell. Syst. Conf.*, 2006, p. 5376.

[5] A. Freedman, D. Rainish, and Y. Gat, "Beam hopping: How to make it possible," in *Proc. Ka Broadband Commun. Conf.*, 2015, pp. 1–5.

[6] M. G. Kibria, E. Lagunas, N. Maturo, D. Spano, and S. Chatzinotas, "Precoded cluster hopping in multi-beam high throughput satellite systems," in *Proc. IEEE Global Commun. Conf. (GLOBECOM)*, Dec. 2019, pp. 1–6.

[7] J. Lei and M. A. Vazquez-Castro, "Multibeam satellite frequency/time duality study and capacity optimization," *J. Commun. Netw.*, vol. 13, no. 5, pp. 472–480, 2011.

[8] *Digital Video Broadcasting (DVB); DVB-S2X Implementation Guidelines for the Second Generation System for Broadcasting, Interactive Services, News Gathering and Other Broadband Satellite Applications—Part 2: S2-Extensions (DVB-S2X)*, document ETSI EN 102 376-2, Jan. 2021.

[9] H. Cao, Y. Su, Y. Zhou, and J. Hu, "QoS guaranteed load balancing in broadband multi-beam satellite networks," in *Proc. IEEE Int. Conf. Commun. (ICC)*. May 2019, pp. 1–6.

[10] P. Zuo, T. Peng, W. Linghu, and W. Wang, "Resource allocation for cognitive satellite communications downlink," *IEEE Access*, vol. 6, pp. 75192–75205, 2018.

[11] Y. Wang *et al.*, "Cooperative beam hopping for accurate positioning in ultra-dense LEO satellite networks," in *Proc. IEEE Int. Conf. Commun. Workshops (ICC Workshops)*, Jun. 2021, pp. 1–6.

[12] R. Alegre-Godoy, N. Alagha, and M. A. Vázquez-Castro, "Offered capacity optimization mechanisms for multi-beam satellite systems," in *Proc. IEEE Int. Conf. Commun. (ICC)*, Jun. 2012, pp. 3180–3184.

[13] L. Chen, E. Lagunas, S. Chatzinotas, and B. Ottersten, "Satellite broadband capacity-on-demand: Dynamic beam illumination with selective precoding," in *Proc. Eur. Signal Process. Conf. (EUSIPCO)*, Dublin, Ireland, Aug. 2021, pp. 900–904.

[14] X. Hu, Y. Zhang, X. Liao, Z. Liu, W. Wang, and F. M. Ghannouchi, "Dynamic beam hopping method based on multi-objective deep reinforcement learning for next generation satellite broadband systems," *IEEE Trans. Broadcast.*, vol. 66, no. 3, pp. 630–646, Sep. 2020.

[15] L. Lei, E. Lagunas, Y. Yuan, M. G. Kibria, S. Chatzinotas, and B. Ottersten, "Beam illumination pattern design in satellite networks: Learning and optimization for efficient beam hopping," *IEEE Access*, vol. 8, pp. 136655–136667, 2020.

[16] X. Yan *et al.*, "The application of power-domain non-orthogonal multiple access in satellite communication networks," *IEEE Access*, vol. 7, pp. 63531–63539, 2019.

[17] A. I. Perez-Neira, M. Caus, and M. A. Vazquez, "Non-orthogonal transmission techniques for multibeam satellite systems," *IEEE Commun. Mag.*, vol. 57, no. 12, pp. 58–63, Dec. 2019.

[18] A. Wang, L. Lei, E. Lagunas, A. I. Pérez-Neira, S. Chatzinotas, and B. Ottersten, "NOMA-enabled multi-beam satellite systems: Joint optimization to overcome offered-requested data mismatches," *IEEE Trans. Veh. Technol.*, vol. 70, no. 1, pp. 900–913, Jan. 2021.

[19] J. Chu, X. Chen, C. Zhong, and Z. Zhang, "Robust design for NOMA-based multibeam LEO satellite Internet of Things," *IEEE Internet Things J.*, vol. 8, no. 3, pp. 1959–1970, Aug. 2021.

[20] J. Jiao, Y. Sun, S. Wu, Y. Wang, and Q. Zhang, "Network utility maximization resource allocation for NOMA in satellite-based Internet of Things," *IEEE Internet Things J.*, vol. 7, no. 4, pp. 3230–3242, Jan. 2020.

[21] A. Wang, L. Lei, E. Lagunas, S. Chatzinotas, A. I. Pérez-Neira, and B. Ottersten, "Joint beam-hopping scheduling and power allocation in NOMA-assisted satellite systems," in *Proc. IEEE Wireless Commun. Netw. Conf. (WCNC)*, Mar. 2021, pp. 1–6.

[22] S. Kisseleff, E. Lagunas, T. S. Abdu, S. Chatzinotas, and B. Ottersten, "Radio resource management techniques for multibeam satellite systems," *IEEE Commun. Lett.*, vol. 25, no. 8, pp. 2448–2542, Aug. 2021.

[23] ESA. *SATellite Network of EXperts (SATNEX) IV*. Accessed: Sep. 8, 2020. [Online]. Available: https://artes.esa.int/projects/satnex-iv

[24] S. Panthi, D. Breynaert, C. McLain, and J. King, "Beam hopping: A flexible satellite communication system for mobility," in *Proc. 35th AIAA Int. Commun. Satell. Syst. Conf.*, 2017, p. 5413.

[25] L. You, D. Yuan, L. Lei, S. Sun, S. Chatzinotas, and B. Ottersten, "Resource optimization with load coupling in multi-cell NOMA," *IEEE Trans. Wireless Commun.*, vol. 17, no. 7, pp. 4735–4749, Jul. 2018.

[26] S. Boyd, S. P. Boyd, and L. Vandenberghe, *Convex Optimization*. Cambridge, U.K.: Cambridge Univ. Press, 2004.

[27] Y.-F. Liu and Y.-H. Dai, "On the complexity of joint subcarrier and power allocation for multi-user OFDMA systems," *IEEE Trans. Signal Process.*, vol. 62, no. 3, pp. 583–596, Feb. 2014.

[28] J. Hartmanis, "Computers and intractability: A guide to the theory of NP-completeness (Michael R. Garey and David S. Johnson)," *Siam Rev.*, vol. 24, no. 1, p. 90, 1982.

[29] A. Zappone, E. Björnson, L. Sanguinetti, and E. Jorswieck, "Globally optimal energy-efficient power control and receiver design in wireless networks," *IEEE Trans. Signal Process.*, vol. 65, no. 11, pp. 2844–2859, Jun. 2017.

[30] K. Shen and W. Yu, "Fractional programming for communication systems—Part I: Power control and beamforming," *IEEE Trans. Signal Process.*, vol. 66, no. 10, pp. 2616–2630, May 2018.

[31] T. Wang and L. Vandendorpe, "Successive convex approximation based methods for dynamic spectrum management," in *Proc. IEEE Int. Conf. Commun. (ICC)*, Jun. 2012, pp. 4061–4065.

[32] S. P. Schurr, D. P. O'Leary, and A. L. Tits, "A polynomial-time interior-point method for conic optimization, with inexact barrier evaluations," *SIAM J. Optim.*, vol. 20, no. 1, pp. 548–571, 2009.

[33] R. Zhao and J. Fan, "Global complexity bound of the Levenberg–Marquardt method," *Optim. Methods Softw.*, vol. 31, no. 4, pp. 805–814, 2016.

[34] J. Lee and S. Leyffer, *Mixed Integer Nonlinear Programming*, vol. 154. Cham, Switzerland: Springer, 2011.

[35] B. Di, L. Song, and Y. Li, "Sub-channel assignment, power allocation, and user scheduling for non-orthogonal multiple access networks," *IEEE Trans. Wireless Commun.*, vol. 15, no. 11, pp. 7686–7698, Nov. 2016.
[36] A. Celik, M.-C. Tsai, R. M. Radaydeh, F. S. Al-Qahtani, and M.-S. Alouini, "Distributed cluster formation and power-bandwidth allocation for imperfect NOMA in DL-HetNets," *IEEE Trans. Commun.*, vol. 67, no. 2, pp. 1677–1692, Feb. 2019.
[37] A. Ginesi, E. Re, and P.-D. Arapoglou, "Joint beam hopping and precoding in HTS systems," in *Proc. Int. Conf. Wireless Satell. Syst.*, Cham, Switzerland: Springer, Sep. 2017, pp. 43–51.
[38] A. I. Aravanis, M. R. S. Bhavani, P. D. Arapoglou, G. Danoy, P. G. Cottis, and B. Ottersten, "Power allocation in multibeam satellite systems: A two-stage multi-objective optimization," *IEEE Trans. Wireless Commun.*, vol. 14, no. 6, pp. 3171–3182, Jun. 2015.
[39] R. M. Karp, "Reducibility among combinatorial problems," in *Complexity of Computer Computations*. Cham, Switzerland: Springer, 1972, pp. 85–103.
[40] P.-D. Arapoglou, K. Liolis, M. Bertinelli, A. Panagopoulos, P. Cottis, and R. De Gaudenzi, "MIMO over satellite: A review," *IEEE Commun. Surveys Tuts.*, vol. 13, no. 1, pp. 27–51, 1st Quart. 2011.



Anyue Wang (Graduate Student Member, IEEE) received the bachelor's and master's degrees in communication engineering from the Beijing University of Posts and Telecommunications (BUPT), Beijing, China, in 2015 and 2018, respectively. He is currently pursuing the Ph.D. degree with the Interdisciplinary Center for Security, Reliability and Trust (SnT), University of Luxembourg, Luxembourg. His research interests include optimization and machine learning for resource management in wireless communication systems.



Lei Lei (Member, IEEE) received the B.Eng. and M.Eng. degrees from Northwestern Polytechnic University, Xi'an, China, in 2008 and 2011, respectively, and the Ph.D. degree from the Department of Science and Technology, Linköping University, Sweden, 2016. He was with the Interdisciplinary Centre for Security, Reliability and Trust (SnT), University of Luxembourg, as a Research Associate and a Research Scientist, from 2016 to 2021. He was a Research Assistant with the Institute for Infocomm Research (I2R), A*STAR, Singapore, in 2013. He is currently an Associate Professor with the School of Information and Communications Engineering, Xi'an Jiaotong University. His current research interests include resource allocation and optimization in terrestrial-satellite networks, energy-efficient communications, and deep learning in wireless communications. He received the IEEE Sweden Vehicular Technology-Communications-Information Theory (VT-COM-IT) Joint Chapter Best Student Journal Paper Award in 2014. He was a co-recipient of the IEEE SigTelCom 2019 Best Paper Award.



Eva Lagunas (Senior Member, IEEE) received the M.Sc. and Ph.D. degrees in telecommunications engineering from the Polytechnic University of Catalonia (UPC), Barcelona, Spain, in 2010 and 2014, respectively. She was a Research Assistant with the Department of Signal Theory and Communications, UPC, from 2009 to 2013. In Summer 2009, she was a Guest Research Assistant with the Department of Information Engineering, Pisa, Italy. From November 2011 to May 2012, she was a Visiting Researcher with the Center for Advanced Communications (CAC), Villanova University, PA, USA. In 2014, she joined the Interdisciplinary Centre for Security, Reliability and Trust (SnT), University of Luxembourg, where she is currently a Research Scientist. Her research interests include radio resource management and general wireless networks optimization.



Ana I. Pérez-Neira (Fellow, IEEE) has been a Full Professor with the Signal Theory and Communication Department, Universitat Politècnica de Catalunya, since 2006, and was a Vice Rector for research (2010–2014). She is currently the Director of the Centre Tecnològic de Telecomunicacions de Catalunya (CTTC). She has more than 60 journal articles and 300 conference papers. She is the coauthor of seven books. She has leaded more than 20 projects and holds eight patents. She is the coordinator of the networks of excellence on satellite communications, financed by the European Space Agency: SatnexIV-V. Her researches are in signal processing for communications, focused on satellite communications. She is a member of the BoG of the IEEE SPS and the vice-president for conferences (2021–2023). She is a member of the Real Academy of Science and Arts of Barcelona (RACAB). She was a recipient for the 2018 EURASIP Society Award and she has been the General Chair of IEEE ICASSP'20 (the first big IEEE virtual conference held by IEEE with more than 15.000 attendees). She has been an Associate Editor of the IEEE TRANSACTIONS ON SIGNAL PROCESSING, *EURASIP SP* and *EURASIP ASP*. Currently, she is a Senior Area Editor of IEEE OPEN JOURNAL OF SIGNAL PROCESSING.



Symeon Chatzinotas (Senior Member, IEEE) is currently a Full Professor/Chief Scientist I and the Head of the SIGCOM Research Group, SnT, University of Luxembourg. He coordinates research activities in communications and networking, acting as a PI in more than 20 projects and is the main representative for 3GPP, ETSI, and DVB. In the past, he was a Visiting Professor with the University of Parma, Parma, Italy, lecturing on 5G wireless networks. He was involved in numerous research and development projects for NCSR Demokritos; CERTH Hellas and CCSR; the University of Surrey, Guildford, U.K. He has coauthored more than 500 technical papers in refereed international journals, conferences, and scientific books. He was a co-recipient of the 2014 IEEE Distinguished Contributions to Satellite Communications Award and the Best Paper Awards at *EURASIP JWCN*, CROWNCOM, ICSSC, and WCNC. He is currently on the Editorial Board Member of the IEEE TRANSACTIONS ON COMMUNICATIONS, IEEE OPEN JOURNAL OF VEHICULAR TECHNOLOGY, and the *International Journal of Satellite Communications and Networking*.



Björn Ottersten (Fellow, IEEE) was born in Stockholm, Sweden, in 1961. He received the M.S. degree in electrical engineering and applied physics from Linköping University, Linköping, Sweden, in 1986, and the Ph.D. degree in electrical engineering from Stanford University, Stanford, CA, USA, in 1990. He has held research positions with the Department of Electrical Engineering, Linköping University; the Information Systems Laboratory, Stanford University; Katholieke Universiteit Leuven, Leuven, Belgium; and the University of Luxembourg, Luxembourg. From 1996 to 1997, he was the Director of research with ArrayComm Inc., a start-up in San Jose, CA, USA, based on his patented technology. In 1991, he was appointed as a Professor of signal processing with the Royal Institute of Technology (KTH), Stockholm. From 1992 to 2004, he was the Head of the Department for Signals, Sensors, and Systems, KTH. From 2004 to 2008, he was the Dean of the School of Electrical Engineering, KTH. He is currently the Director of the Interdisciplinary Centre for Security, Reliability and Trust, University of Luxembourg. As a Digital Champion of Luxembourg, he acts as an Adviser to the European Commission. He is a fellow of EURASIP. He was a recipient of the IEEE Signal Processing Society Technical Achievement Award in 2011 and the European Research Council Advanced Research Grant twice (2009–2013 and 2017–2022). He has coauthored journal articles that received the IEEE Signal Processing Society Best Paper Award in 1993, 2001, 2006, and 2013, and seven other IEEE conference papers best paper awards. He has served as the Editor-in-Chief for *EURASIP Journal on Advances in Signal Processing*, an Associate Editor for the IEEE TRANSACTIONS ON SIGNAL PROCESSING, and the Editorial Board Member of the *IEEE Signal Processing Magazine*. He is currently a member of the editorial boards of *EURASIP Journal on Advances in Signal Processing* and *Foundations and Trends of Signal Processing*.